AIP Advances

# Photoluminescence at room temperature of liquid-phase crystallized silicon on glass

Cite as: AIP Advances **6**, 125004 (2016); https://doi.org/10.1063/1.4971279
Submitted: 28 July 2016 • Accepted: 17 November 2016 • Published Online: 05 December 2016

**Michael Vetter, Anka Schwuchow and Gudrun Andrä**

ARTICLES YOU MAY BE INTERESTED IN

Strong out-of-plane magnetic anisotropy in ion irradiated anatase $TiO_2$ thin films
AIP Advances **6**, 125009 (2016); https://doi.org/10.1063/1.4971794

Photoluminescence imaging of silicon wafers
Applied Physics Letters **89**, 044107 (2006); https://doi.org/10.1063/1.2234747

Terahertz detectors from Be-doped low-temperature grown InGaAs/InAlAs: Interplay of annealing and terahertz performance
AIP Advances **6**, 125011 (2016); https://doi.org/10.1063/1.4971843

Read Now!
AIP Advances
Biophysics & Bioengineering Collection

AIP Publishing



© 2016 Author(s).

AIP ADVANCES **6**, 125004 (2016)

# Photoluminescence at room temperature of liquid-phase crystallized silicon on glass

Michael Vetter, Anka Schwuchow, and Gudrun Andrä
*Leibniz-Institute of Photonic Technology (IPHT), Albert-Einstein-Str. 9, D-07745 Jena, Germany*

(Received 28 July 2016; accepted 17 November 2016; published online 5 December 2016)

The room temperature photoluminescence (PL) spectrum due band-to-band recombination in an only 8 μm thick liquid-phase crystallized silicon on glass solar cell absorber is measured over 3 orders of magnitude with a thin 400 μm thick optical fiber directly coupled to the spectrometer. High PL signal is achieved by the possibility to capture the PL spectrum very near to the silicon surface. The spectra measured within microcrystals of the absorber present the same features as spectra of crystalline silicon wafers without showing defect luminescence indicating the high electronic material quality of the liquid-phase multi-crystalline layer after hydrogen plasma treatment. © *2016 Author(s). All article content, except where otherwise noted, is licensed under a Creative Commons Attribution (CC BY) license (http://creativecommons.org/licenses/by/4.0/).* [http://dx.doi.org/10.1063/1.4971279]

Laboratory solar cells implementing very thin about 10 to 20 μm thick liquid-phase crystallized silicon on glass (LPCSG) produced by line focus laser beam or electron beam (e-beam) crystallization of amorphous and nanocrystalline silicon layers on glass, showed open circuit voltages ($V_{oc}$) of 656 mV[1–6] comparable to industrial and highest efficient multi-crystalline wafer solar cells.[7] Therefore, LPCSG presents a promising material to fabricate solar cells and modules. This technology could merge the advantage of crystalline silicon (c-Si) wafer technology with its high efficiency potential and thin film technology with low Si consumption and low cost monolithic integration for module fabrication. LPCSG technology could be an approach to overcome the emerging limits for further cost reduction in standard wafer-based module technology. Most developments of the LPCSG absorbers have been made by fabricating solar cells, measuring and analyzing their current-voltage (IV) characteristics and quantum efficiency (QE) or on quasi-solar cells measuring the Suns-$V_{oc}$ characteristic. For detailed characterization of material properties of multi-crystalline (mc) silicon wafers photoluminescence (PL) imaging using CCD cameras has been developed in recent years[8] and is becoming new standard of wafer inspection in solar cell industry. This technique has been shown to detect also the photoluminescence of very thin silicon absorbers by implementing several modifications to standard equipment.[9] However, it was not possible to correlate quantitatively the PL images with material properties of LPCSG absorbers. Recently, the measurement of the effective charge carrier lifetime ($\tau_{eff}$) in LPSCG absorbers using the quasi steady-state photoconductance method (QSS-PC)[10] was introduced to determine the absorber quality already after the laser crystallization process.[11] This gives an early and immediate feedback of the quality of solar cell precursors in every fabrication step and accelerates the solar cell process development. However, the injection level dependent photoconductance data gives average values, e.g. of the $\tau_{eff}$ and the implied open circuit voltage ($V_{oc}$), over a sample area of several square centimeters, but gives no detailed data of small areas as e.g. crystal grains in mc-Si material. It would be very interesting to measure the effective lifetime in thin film mc-Si layers also directly by PL, since e.g. trapping of charge carriers has less impact on PL measurements.[12] With the objective to further develop the PL technique for this purpose we present the measurement of photoluminescence at room temperature of very thin about 8 μm thick mc Si layers on glass in this paper.

For all photoluminescence measurements we use the experimental setup shown in Fig. 1(a). The setup basically consists of a SDL tunable laser diode (≈ 200 mW) at 817 nm (focused beam diameter 1-2 mm) for optical excitation and a cleaved optical fiber (400 μm diameter) which is collecting the

 © Author(s) 2016

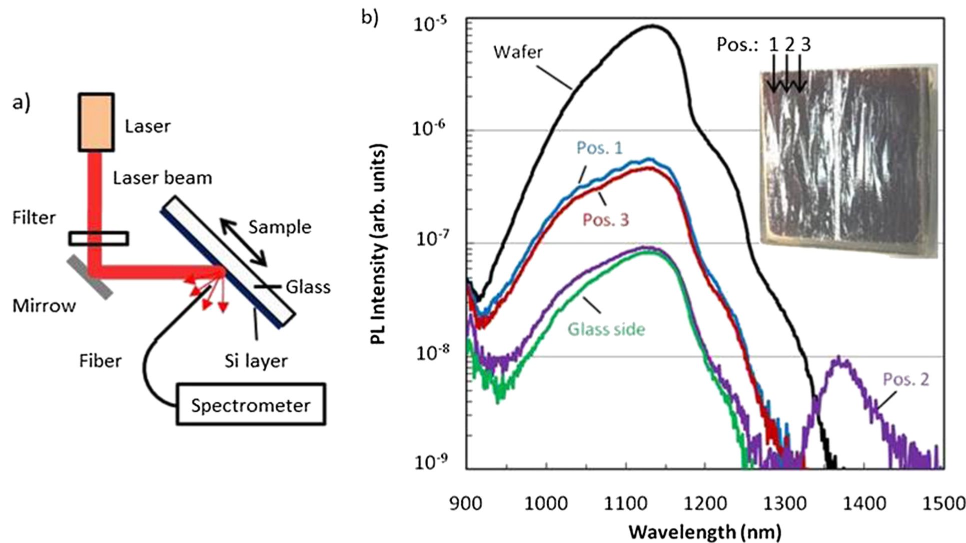


FIG. 1. (a) Implementation of a thin (400 µm) optical fiber permits to detect the PL very near to the Si surface (distance less than 1 mm) which results in a very high PL signal and high spatial resolution. (b) Comparison of the room temperature PL spectrum of a n-type 675 µm thick Si wafer with the spectra at different positions of an 8 µm thick n-type LPC mc Si layer. The insert shows the LPCSG absorber (2.5 cm x 2.5 cm) from the top side (Si layer) with an indication of the (approx.) position of the PL measurements.

PL just from the excited sample surface and guides it directly to a Spectro 320 fiber spectrometer (Instrument Systems). To suppress the long wavelength part of the emission band of the laser diode that is overlapping with the PL-wavelength region of the sample, the excitation beam is filtered by a short pass filter (FES850, Thorlabs). The implementation of an optical fiber permits to detect the PL very near to the silicon surface (distance less than 1 mm) which results in a very high PL signal that can be detected without any lock-in amplifying technology.

Fig. 1(b) compares the room temperature PL spectrum of a n-type (1.5 Ωcm, $N_D = 3x10^{15}$ $cm^{-3}$, orientation <100>) 675 µm thick Si wafer electronically passivated on both sides by an intrinsic amorphous Si (i-Si) layer and the PL spectra at different positions of an 8 µm thick n-type (0.1 Ωcm) liquid-phase crystallized (LPC) silicon layer passivated on the front side by a hetero emitter structure consisting of an (≈ 10 nm thick) i-Si layer and a p-type amorphous Si layer (p-Si, ≈ 30 nm thick). The LPC Si layer is deposited by electron beam evaporation on a sputtered silicon oxide/silicon oxide nitride buffer layer stack on 3 mm Borofloat 33 glass (Schott). The LPC Si film is crystallized by an 808 nm continuous wave line focus laser (LIMO Lissotschenko Mikrooptik GmbH), afterwards hydrogen plasma passivation of electronic defects and a surface etch treatment has been performed then the hetero emitter was deposited.[11] In Fig. 1(b) is included a photo of the LPCSG sample with an indication of the different measurement positions of the spectra. In our measurement procedure for the PL spectra, first we use a common Si wafer, known for its strong PL signal, to adjust the position of the excitation beam focus on the sample as well as the position and the optimal incident angle of the optical fiber to collect maximum PL intensity. The black line in Fig. 1(b) represents the PL-spectrum of a Si-wafer showing the typical spectral PL emission of c-Si with a peak at about 1100 nm (1.1 eV) of the radiation due to band to band recombination in Si.[13] Then, we exchange the wafer by the LPCSG sample with the Si layer showing to the optical fiber. Different structures occurring in LPCSG layers (crystallites, grain boundaries) were precisely placed in the focus of the excitation beam to measure their specific PL-spectra. In Fig. 1(b) the PL-spectra from different positions, respectively structures, at the LPCSG layer are depicted. The blue curve (Pos. 1) and the red curve (Pos. 3) show PL spectra taken at two different large crystallites with size in the range of approx. 10 mm x 1 mm as measured in an amplified picture of the sample. The interference fringes, which are located on the low wavelength side of the maximum PL intensity of the blue curve (Pos. 1), result from internal reflections in the thin Si film. Interference fringes are not very pronounced due

to low coherence of the PL light however, they can be used to calculate the thickness of the Si film. From Young's equation results the layer thickness (d) by $d = (\lambda_1 * \lambda_2)/(2n\Delta\lambda)$, where $\lambda_1$ and $\lambda_2$ are the wavelengths of two adjacent maxima in the spectrum, $\Delta\lambda$ is the difference in wavelength of the maxima and n is the refractive index of Si. Taking the respective values of four maxima from the top part of the spectrum measured at Pos. 1 results in an average value of about 8 µm. This coincides well with the expected thickness of the sample after surface etch (initial thickness was 10 µm). At the second crystal grain (Pos. 3), interference fringes in the PL spectrum are not very pronounced. We suppose that the crystal orientation is different from that at Pos. 1 and due to surface etching the crystal surface is slightly tilted to that of Pos. 1 resulting in damping the interference effect. At Pos. 2 of the photo we are located at several grain boundaries resulting in the purple curve presented in Fig. 1(b). The maximum PL-intensity is about five times lower than for the large crystallites and a second emission band between 1300 nm and 1500 nm appears. Latter emission is attributed to defect luminescence and is reported for solid phase crystallized silicon layers[14] and for electron beam crystallized silicon layers at low temperatures.[15] Finally, the sample was turned, illuminated and the PL was measured in a large crystallite from the glass side (Fig. 1(b) green curve). Illuminating and measuring from the glass side the detector signal is about one order of magnitude lower than from the silicon side. We assume that this is mainly due to the fact that the distance between the optical fiber and the silicon surface is larger since the 3 mm thick substrate glass is in between. Therefore, the collection efficiency of the fiber is lower.

To validate our data, in Fig. 2(a) we compare the PL spectrum of our 675 µm thick i-Si passivated wafer with a recently published PL spectrum of a 200 µm thick silicon nitride ($SiN_x$) passivated wafer[16] (purple circles) and measured at 300 K. In Ref. 16 the PL spectrum is normalized to the maximum PL intensity situated at the Si band gap energy of 1.1 eV. In addition, the spectrum has been corrected for reabsorption of emitted radiation in the Si wafer. To calculate the amount of reabsorbed photons also in our samples, the following procedure described in Ref. 13 was applied. The generation rate ($\delta g_{sp}$) of photons per volume and energy interval in a semiconductor is given by the generalized Planck law:[17–19]

$$\delta g_{sp} = (8\pi\, n^2/h^3 co^2)(h\nu)^2\, \alpha_{BB}\, e^{(-h\nu/kT)}\, e^{(\Delta EF/kT)}\, \delta(h\nu) \quad (1)$$

with n the refractive index, h the Planck constant, $c_0$ the speed of light in vacuum, ν the wavelength, $\alpha_{BB}$ the band-band absorption coefficient (depending on hν), k the Boltzmann constant, T the absolute temperature and $\Delta_{EF}$ the quasi Fermi level splitting under illumination. The photoluminescence

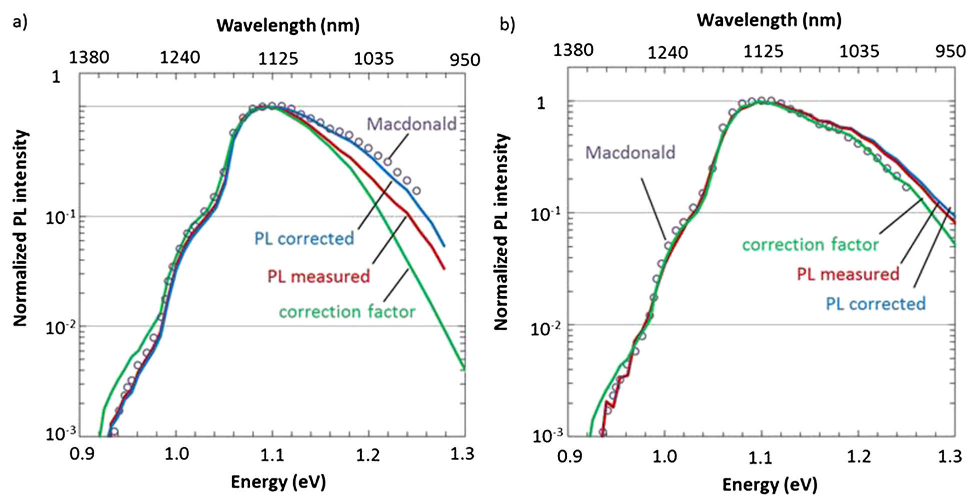


FIG. 2. (a) Comparison of the room temperature PL spectrum of an n-type 675 µm thick Si wafer (blue curve: corrected for reabsorption, red curve: as measured) with the PL data of Macdonald[16] (purple dots). The green curve represents the correction function used to calculate the corrected spectrum for the wafer by Eq. 3. (b) Comparison of the room temperature PL spectrum of an n-type 8 µm thick LPCSG absorber with the PL data of Macdonald. The green curve represents the correction function to calculate the corrected spectrum for the 8 µm thick Si layer by Eq. 3.

emitted from a plan-parallel sample as a Si wafer can be calculated from Eq. 1 by integrating over the sample thickness d, in addition one has to consider the amount of photons reabsorbed in the sample ($A_{re}$). For such a planar sample illuminated by monochromatic light, PL is given by:[17,20–22]

$$PL = \delta g_{sp} A_{re} / 4\,\alpha_{BB}\, n^2 = [2\pi/(h^3 co^2)](h\nu)^2 A_{re}\, e^{(-h\nu/kT)}\, e^{(\Delta EF/kT)}\, \delta(h\nu) \quad (2)$$

where the absorptivity of the sample, $A_{re}$ (as function of hν), is approximated by the following equation considering multiple reflections between two surfaces:

$$A_{re}(h\nu) = [1 - R_F(h\nu)][1 - e^{(-\alpha BB(h\nu)^* d)}][1 + R_B(h\nu) e^{(-\alpha BB(h\nu)^* d)}]/[1 - R_F(h\nu) R_B(h\nu)\, e^{(-2^* \alpha BB(h\nu)^* d)}] \quad (3)$$

with $R_F(h\nu)$ and $R_B$ (hν) the reflection of the sample front side and back side, respectively.

Eq. 3 is the solution resulting from the generalized Planck law for the case that the excess carrier density (Δn) is homogenous over the wafer thickness and therefore $\Delta_{EF}$ is constant, and so is $e^{(\Delta EF/kT)}$. This is only true for a Si sample where the carrier diffusion length is larger than the wafer thickness and the surface recombination velocity is very low. To prove this for our samples, the effective carrier lifetime of the c-Si wafer and the LPCSG absorber was determined by the QSS-PC method. For the c-Si wafer results $\tau_{eff} \approx 1$ ms at 1 Sun illumination intensity, corresponding to a diffusion length ($L_{eff}$) of about $L_{eff} \approx 1$ mm, larger than the wafer thickness. This indicates a very good surface passivation with a low surface recombination velocity resulting in a homogenous charge carrier profile under illumination. At the high injection level of the laser irradiation (≈ 200 mW/0,02 $cm^2$ = 100 Suns) $\tau_{eff}$ is in the range of only 10 µs ($L_{eff} \approx 100$ µm) due to Auger recombination. Nonetheless, the injection profile remains homogenous over the sample thickness since Auger recombination is homogenously distributed. For the LPCSG absorber we measured $\tau_{eff}$ for injection levels higher than 50 Suns resulting in a $\tau_{eff}$ (100 Suns) ≈ 35 ns (excess carrier density, $\Delta n \approx 4x10^{14}$ $cm^{-3}$) corresponding to a $L_{eff}$ of about 5 µm less than the absorber thickness. The lifetime data indicates that carrier lifetime is dominated by the surface recombination at one or both sample sides and we cannot assume a homogenous charge carrier profile under high laser illumination. Under this condition $\Delta_{EF}$ is not constant, which makes the calculation of the amount of reabsorbed photons very complex.

In Fig. 2(a) the normalized measured PL spectrum of our 675 µm thick wafer from Fig. 1(b) is presented by the red curve. The green curve represents the normalized correction function CF(hν) calculated by Eq. 3 and multiplying $A_{re}(h\nu)$ by the factor $PF = (h\nu)^{2*} e^{(-h\nu/kT)}$. For the calculation of $A_{re}$ the reflection of the samples was measured with a spectrometer with integrating sphere (Lambda 900, PerkinElmer). The CF curve describes the relative increase of the absorption coefficient by the reabsorption effect and is more pronounced for high energy photons due to their larger absorption coefficient. The corrected PL spectrum in Fig. 2(a) shown by the blue curve is then calculated by $PL_{cor}$= [(PL/PF) (1 + $A_{re}(h\nu)$)] PF and normalizing again.

Our corrected PL data lies in the low and high energy range slightly under the data from Ref. 16 which is supposed to mainly result from not exactly same sample temperature. Our sample was not mounted on a temperature controlled sample stage and was about 293 K, the laboratory temperature. In addition, the digitalization of data from Ref. 16 and of the absorption coefficient from Ref. 13 might introduce an error.

Fig. 2(b) compares the normalized PL spectrum of the LPCSG absorber from Pos. 1 in Fig. 1(b) with the data of Ref. 16. Here the green curve presents the correction function calculated for a thin Si layer of 8 µm thickness. The CF coincides with the corrected PL spectrum from Ref. 16 and the correction of our measured data is very small. One concludes that in an 8 µm thick sample reabsorption has only a small impact on the PL signal in the here presented data range. Interestingly, the PL intensity at high energies is relatively higher for the thin LPCSG absorber than for a wafer, which is also found for other LPCSG absorber in this thickness range. Probably the non-homogeneous excess carrier (Δn) distribution is responsible for this effect. This could be detected e.g. by illuminating with different wavelengths. For non-homogenous Δn Eq. 3 in principle is not valid and the exponential factor $e^{(\Delta EF/kT)}$ in Eq. 2 might introduce an additional dependence of the PL on wavelength. However, the calculation of this sample configuration is very complex and is out of the scope of this work.

In conclusion, we have measured the room temperature photoluminescence spectrum due band to band recombination in a lightly doped n-type crystalline silicon wafer with a thin 400 μm thick optical fiber directly coupled to the spectrometer. Using an optical fiber allows to collect the emitted photoluminescence radiation very near to the wafer surface resulting in an excellent signal without the need to amplify the detector signal by lock-in technology. The spectrum has been corrected by reabsorption and coincides well with data reported in literature. Next, we used the experimental setup to measure for the first time the room temperature photoluminescence spectrum in several microcrystals of a thin 8 μm n-type liquid-phase crystallized silicon layer on glass. Due to the small layer thickness, the radiation from the microcrystals is about 10 times lower than of the silicon wafer nevertheless, spectra could be measured over three orders of magnitude. The spectra measured within the area of microcrystals present the same features as the spectrum of the silicon wafer without showing defect luminescence indicating the high electronic material quality of the mc Si layer after hydrogen plasma treatment. Defect luminescence was found when measuring at grain boundaries, however with emission intensity usually lower than the band to band emission, also an indication of the high material quality. Interestingly, the relative photoluminescence emission at high energies of thin mc Si layers is higher than in a thick wafer, which is still under investigation. The photoluminescence of the thin mc Si layer also could be measured through the 3 mm thick Borofloat 33 glass substrate but with about 10 times lower signal. It shows that optical fiber technology together with photoluminescence detection is a very promising technology for material and process control of thin silicon solar cells. This kind of equipment e.g. can be further developed to perform time-resolved measurements of PL intensity e.g. generated by pulsed laser light. This will give information on carrier lifetime and recombination mechanisms in the Si layers. Furthermore, the simulation and fitting of PL spectra with theoretical curves using phonon absorption and emission bands in Si can give information e.g. on doping density in thin mc Si layers but also on density of states of phonons in Si in general.[16]

One of the authors (M.V.) has received funding from the European Union's Horizon 2020 research and innovation programme under the Marie Sklodowska-Curie grant agreement No. 657115 (cSiOn-Glass). We like to thank the Thüringer Aufbaubank (TAB) and the European Commission (ESF) for funding the project Bi-PV (FKZ 2015 FGR 0078).

[1] J. Haschke, D. Amkreutz, L. Korte, F. Ruske, and B. Rech, Solar Energy Mater. Solar Cells **128**, 190 (2014).
[2] P. Sonntag, J. Haschke, S. Kühnapfel, T. Frijnts, D. Amkreutz, and B. Rech, Prog. Photovolt. Res. Appl. **24**, 716 (2016).
[3] J. Dore, D. Ong, S. Varlamov, R. Egan, and M. A. Green, IEEE J. Photovolt. **4**, 33 (2014).
[4] A. Gawlik, I. Höger, J. Bergmann, J. Plentz, T. Schmidt, F. Falk, and G. Andrä, Phys. Status Solidi RRL **9**, 397 (2015).
[5] G. Jia, G. Andrä, A. Gawlik, S. Schönherr, J. Plentz, B. Eisenhawer, T. Pliewischkies, A. Dellith, and F. Falk, Sol. Energy Mater and Solar Cells **126**, 62 (2014).
[6] M. Junghanns, J. Plentz, G. Andrä, A. Gawlik, I. Höger, and F. Falk, Appl. Phys. Lett. **106**, 083904 (2015).
[7] M. A. Green, K. Emery, Y. Hishikawa, W. Warta, and E. D. Dunlop, Progr. Photovol. Res. Appl. **24**, 905 (2016).
[8] www.btimaging.com/
[9] A. Teal, J. Dore, and S. Varlamov, Solar Energy Mat. Solar Cells **130**, 1 (2014).
[10] R. A. Sinton and A. Cuevas, Appl. Phys. Lett. **69**, 457 (1996).
[11] M. Vetter, A. Gawlik, J. Plentz, G. Andrä, Energy Procedia (2016) accepted for publication.
[12] R. A. Bardos, T. Trupke, M. C. Schubert, and T. Roth, Appl. Phys. Lett. **88**, 053504 (2006).
[13] H. T. Nguyen, F. E. Rougieux, B. Mitchell, and D. Macdonald, J Appl. Phys. **115**, 043710 (2014).
[14] T. Mchedlidze, J. Schneider, T. Arguirov, and M. Kittler, Phys. Status Solidi **C8**, 1334 (2011).
[15] W. Seifert, D. Amkreutz, T. Arguirov, M. Krause, M. Schmidt, Solid State Phenomena **178-179**, 116 (2011).
[16] D. Macdonald, A. Y. Liu, H. T. Nguyen, S. Y. Lim, R. E. Rougieux, Proc. 31st EU PVSEC Hamburg (2015), 440.
[17] P. Würfel, J. Phys. C **15**, 3967 (1982).
[18] P. Würfel, S. Finkbeiner, and E. Daub, Appl. Phys. A: Mater. Sci. Processs. **60**, 67 (1995).
[19] P. Würfel, T. Trupke, T. Puzzer, E. Schäffer, W. Warta, and S. W. Glunz, J. Appl. Phys. **101**, 123110 (2007).
[20] E. Daub and P. Würfel, Phys. Rev. Lett. **74**, 1020 (1995).
[21] T. Trupke, M. A. Green, P. Würfel, P. P. Altermatt, A. Wang, J. Zhao, and R. Corkish, J. Appl. Phys. **94**, 4930 (2003).
[22] T. Trupke, E. Daub, and P. Würfel, Solar Energy Mater. Solar Cells **53**, 103 (1998).